



Sulfur isotopic composition of individual organic compounds from Cariaco Basin sediments



Morgan Reed Raven^{a,*}, Jess F. Adkins^a, Josef P. Werne^b, Timothy W. Lyons^c, Alex L. Sessions^a

^a Division of Geological and Planetary Sciences, California Institute of Technology, Pasadena, CA 91125, USA

^b Geology and Planetary Science, University of Pittsburgh, Pittsburgh, PA 15260, USA

^c Department of Earth Sciences, University of California, Riverside, CA 92521, USA

ARTICLE INFO

Article history:

Received 13 February 2014

Received in revised form 22 December 2014

Accepted 7 January 2015

Available online 14 January 2015

Keywords:

Sulfur isotopes

Organosulfur compounds

Sediment diagenesis

Kerogen

Cariaco Basin

ABSTRACT

Reactions between reduced inorganic sulfur and organic compounds are thought to be important for the preservation of organic matter (OM) in sediments, but the sulfurization process is poorly understood. Sulfur isotopes are potentially useful tracers of sulfurization reactions, which often occur in the presence of a strong porewater isotopic gradient driven by microbial sulfate reduction. Prior studies of bulk sedimentary OM indicate that sulfurized products are ³⁴S-enriched relative to coexisting sulfide, and experiments have produced ³⁴S-enriched organosulfur compounds. However, analytical limitations have prevented the relationship from being tested at the molecular level in natural environments. Here we apply a new method, coupled gas chromatography – inductively coupled plasma mass spectrometry, to measure the compound-specific sulfur isotopic compositions of volatile organosulfur compounds over a 6 m core of anoxic Cariaco Basin sediments. In contrast to current conceptual models, nearly all extractable organosulfur compounds were substantially depleted in ³⁴S relative to coexisting kerogen and porewater sulfide. We hypothesize that this ³⁴S depletion is due to a normal kinetic isotope effect during the initial formation of a carbon–sulfur bond and that the source of sulfur in this relatively irreversible reaction is most likely the bisulfide anion in sedimentary porewater. The ³⁴S-depleted products of irreversible bisulfide addition alone cannot explain the isotopic composition of total extractable or residual OM. Therefore, at least two different sulfurization pathways must operate in the Cariaco Basin, generating isotopically distinct products. Compound-specific sulfur isotope analysis thus provides new insights into the time-scales and mechanisms of OM sulfurization.

© 2015 Elsevier Ltd. All rights reserved.

1. Introduction

Organic matter (OM) is preserved in sediments as a complex macromolecular structure known as kerogen. However, many of the mechanisms for forming kerogen are poorly understood (Francois, 1987; Eglinton et al., 1994; Aizenshtat et al., 1995; Vandenbroucke and Largeau, 2007). Organic compounds are sometimes bound to the kerogen matrix by sulfur bridges, and organic sulfur in a variety of aromatic and aliphatic ring structures can also be extracted from immature sediments (Vairavamurthy and Mopper, 1987; Vairavamurthy et al., 1994; Sinninghe Damsté et al., 2007) and crude oils (e.g. Schmid et al., 1987; Sinninghe Damsté et al., 1987; Sinninghe Damsté and De Leeuw, 1990). Although some of the organic sulfur compounds (OSCs) in marine sediments have been reproduced under laboratory conditions

(LaLonde et al., 1987; de Graaf et al., 1992; Rowland et al., 1993; Schouten et al., 1994; Kok et al., 2000; Amrani and Aizenshtat, 2004a,b), the relationship between sulfurization reactions in natural systems and the sulfur isotopic composition of sedimentary OM has not been determined.

Organic sulfur (OS) in kerogen or proto-kerogen, which we refer to as 'residual' OS, is typically more enriched in ³⁴S than its likely sulfur sources, either bisulfide or polysulfide species in coexisting porewater (Anderson and Pratt, 1995; Bottrell and Raiswell, 2000). The phenomenon has been difficult to explain on the basis of experimental (Amrani and Aizenshtat, 2004a) and initial compound-specific $\delta^{34}\text{S}$ results (Werne et al., 2008). Moreover, only a subset of available functionalized organic compounds are affected by sulfurization, while others persist in sediments without experiencing sulfurization. In this study, we have investigated whether sulfur isotopes can provide a tracer for mechanisms of OS formation at the molecular level. We use a newly developed method for compound-specific sulfur isotope analysis (Amrani et al.,

* Corresponding author. Tel.: +1 (626) 395 8647.

E-mail address: mrraven@caltech.edu (M.R. Raven).

2009) to obtain $\delta^{34}\text{S}$ values for individual, GC-amenable organosulfur compounds (OSCs) from Cariaco Basin sediments.

Sulfur isotopic composition is a potentially powerful tool for exploring the timing and mechanisms of organic sulfurization reactions due to the large downcore porewater sulfur isotope gradient typically generated by microbial sulfate reduction in anoxic sediments. The sulfur isotopic composition of bulk pools has been used to constrain the timing of kerogen and extractable OSC formation relative to pyrite and other sedimentary sulfur sinks. However, because OSCs form at different rates and during various stages of early diagenesis (Vairavamurthy and Mopper, 1987; Vairavamurthy et al., 1994; Sinninghe Damsté et al., 2007; Werne et al., 2008), bulk OS potentially represents a mixture of OSCs with diverse $\delta^{34}\text{S}$ values. Our results represent the first $\delta^{34}\text{S}$ measurements for individual OSCs in complex lipid extracts from marine sediments.

2. Site background

Samples were taken from the Cariaco Basin, north of Venezuela. The water column is anoxic and sulfidic below 300 m, which facilitates the delivery of a moderately high concentration of reduced inorganic sulfur species and organic carbon (up to 6 wt%) to the sediments, making the site an excellent one for studying organic sulfurization reactions. Sample material was obtained from Ocean Drilling Program (ODP) Core 1002B from the western side of Cariaco Basin at Site 165 at ca. 900 m water depth (Shipboard Scientific Party, 1997). The core was frozen immediately following collection, with the exception of the shallowest material (40 cm sample), which was squeezed to extract porewater onboard and then frozen. The core has been stored frozen since then. Subsamples (8) from the core were obtained from the frozen archive in 2011, and 3 additional subsamples were collected in 2012. The subsamples each represented ca. 2 cm of homogenized material and were spaced at 8 roughly equal depth intervals between 40 and 535 cm, all within the upper laminated section of the core that appears to have experienced continuous anoxic and sulfidic deposition (Lyons et al., 2003). Our deepest sample was near the contact with underlying massive sediments at ca. 650 cm and represented nearly 12.6 ^{14}C kyr (14.5 calendar kyr) of deposition. The age model for the core is based on correlation of magnetic susceptibility with a nearby core (PL07-39PC) that had been well-dated using radiocarbon (Lin et al., 1997; Werne et al., 2000).

The lithology and geochemistry of Core 1002B have been studied extensively, providing a valuable context for our work. Werne et al. (2003) presented depth profiles of the concentration and sulfur isotopic composition of pyrite, reactive iron, extractable OS ('bitumen'), residual OS ('kerogen'), total sulfur and porewater SO_4^{2-} and HS^- . Other available data for the core included concentration of organic and inorganic C, Mo, Fe and Al (Lyons et al., 2003), and major biomarker distributions (Werne et al., 2000).

Porewater SO_4^{2-} concentration in the basin declines steadily from > 27 mM at the sediment–water interface to 3.8 mM by 590 cm depth. Porewater HS^- concentration increases from a water column-like concentration of < 0.1 mM near the surface to 9.0 mM at 215 cm and then decreases below. Both SO_4^{2-} and HS^- become progressively ^{34}S -enriched in deeper sediments, a common pattern associated with distillation of the porewater sulfate reservoir by dissimilatory microbial SO_4^{2-} reduction (LaLonde et al., 1987; de Graaf et al., 1992; Rowland et al., 1993; Schouten et al., 1994; Kok et al., 2000; Werne et al., 2003; Amrani and Aizenshtat, 2004a,b). Pyrite sulfur is present at ca. 1.3 wt% in surface sediments. Deeper diagenetic pyrite formation is relatively minor and likely Fe-limited. Throughout the profile, pyrite is similar in its $\delta^{34}\text{S}$ values to water column HS^- and is ^{34}S -depleted

relative to both coexisting HS^- and kerogen, which is consistent with early formation of pyrite, including formation in the water column (Aizenshtat et al., 1995; Anderson and Pratt, 1995; Lyons et al., 2003). OM is abundant [up to 6 wt% total organic carbon (TOC)] and sulfur rich (up to 0.6 wt% kerogen S; Werne et al., 2003). OSCs have also been observed in the extractable lipid fraction below 240 cm (Werne et al., 2000).

3. Methods and instrumentation

The data were collected iteratively, as separation and analytical methods were incrementally improved over the course of the study (described below). In all cases, frozen sediment (2–5 g) was dried under vacuum and free lipids were obtained by microwave extraction at 100 °C for 15 min (Mars 5, CEM Corp.) in 9:1 v/v dichloromethane (DCM):MeOH. Compounds were separated via polarity on a silica gel column (4 g) by sequential elution with 4:1 hexane:DCM (F1, 40 ml, all depths), DCM (F2, 40 ml, for 40, 70, 265 and 535 cm depths only) and 1:1 DCM:MeOH (F3, 40 ml, all depths). Initial analysis with gas chromatography (GC) was conducted with a Varian CP-3800 GC instrument equipped with a HP DB5-MS (30 m \times 320 μm i.d. \times 0.25 μm film) column and programmed temperature vaporization (PTV) injector. GC effluent was split between a Varian Saturn 2200 ion trap mass spectrometer with electron impact (EI) ionization and a Sievers 355 sulfur chemiluminescence detector (SCD) for simultaneous identification and quantification of OSCs.

3.1. Compound-specific ^{34}S analysis using GC-ICPMS

The sulfur isotopic composition of individual GC-amenable organic compounds from all fractions was measured using multi-collector inductively-coupled plasma mass spectrometry (MC-ICPMS; Thermo Neptune⁺) an Agilent 6890 GC instrument for gas-phase sample introduction and separation following the approach described by Amrani et al. (2009). This GC instrument was operated with the same column type and operating conditions as the Varian instrument but differed in that it had a split/splitless injector. Accuracy was established by repeated analysis of external standard mixtures containing three to six OSCs with known $\delta^{34}\text{S}$ values. Mean $\delta^{34}\text{S}$ values for the combined data for each standard were within 1.4‰ of published EA-IRMS values (Amrani et al., 2009) and had a root-mean-squared variance of 1.5‰. Due to improvements in chromatography and baseline standardization, the 2012 data are all accurate to within 1.0‰ and have a root-mean-squared variance of 0.9‰. Many of the polar fractions (F3, see below) of the extracts were analyzed in triplicate to assess any additional uncertainty due to the complexity of the chromatograms. Triplicate analyses for most of the major peaks in F3 achieved a $\delta^{34}\text{S}$ standard deviation of 1.3–1.8‰, although several peaks with less well resolved baselines returned a wider range of values. F2 chromatograms were much less crowded and $\delta^{34}\text{S}$ values for duplicate F2 runs varied by a maximum of 0.8‰. This performance is comparable with that reported by Amrani et al. (2009, 2012) for complex environmental samples.

A gas phase standard (SF_6) with known $\delta^{34}\text{S}$ value was used for tuning and calibration of isotope ratio values. In our earliest analyses, the Ar 'sample gas' for the plasma was preheated by flowing through the GC oven before entering the custom-built heated transfer line. With this arrangement, both sensitivity and $\delta^{34}\text{S}$ values drifted systematically (by nearly 10‰ in the latter case) as the GC oven was ramped from 80–300 °C. We now understand that this effect arises from an imperfect response of the Neptune mass flow controllers to changing flow resistance with GC oven temperature. To account for such effects, sample $\delta^{34}\text{S}$ values were

standardized to a linear interpolation of frequent SF₆ reference gas peaks (Supplemental Fig. 1). In later analyses, we eliminated this drift by isolating the sample gas heating system from the GC oven. In this system, the Ar flow was preheated to a constant 320 °C outside the GC oven before entering the upstream end of the transfer line to the plasma torch. An additional heating tape was also added at the ground glass connection between the transfer line and the injector torch to improve the transfer of higher-boiling-point analytes into the plasma. With these modifications, good peak shape was obtained for compounds eluting at oven temperatures of up to 300 °C, permitting sulfur isotopic analysis of a wider range of GC-amenable compounds. Because $\delta^{34}\text{S}$ values for SF₆ drifted by < 1‰ across the GC temperature program under these conditions, drift correction was no longer necessary and standard peaks were not required in the midst of the GC oven temperature program, thus avoiding potential interference between standard and analyte peaks.

GC-ICPMS data were exported from the Neptune Evaluation software into Isodat v. 3.1 (Thermo) for processing. Results are reported in the conventional $\delta^{34}\text{S}$ notation as permil (‰) deviation from the VCDT standard. Accurate and precise $\delta^{34}\text{S}$ values were obtained for analytes producing peak areas of at least 1 Vs, representing ca. 50 pmol of analyte on-column. Unlike for other light isotopes (H, C, N), we have not observed chromatographic separation of sulfur isotopologues, meaning that ³⁴S/³²S ratio values are invariant across even large chromatographic peaks. This is consistent with previous observations (Amrani et al., 2009, 2012). Poor chromatographic peak shapes and/or coelution were the dominant source of measurement uncertainty, particularly during early analyses. Results were sometimes moderately sensitive to the manually selected background interval due to the contribution of unresolved OSCs to the *m/z* 34/32 ratio of background signals, and peaks for which $\delta^{34}\text{S}$ values varied by > 1.5‰ for alternative baseline definitions were discarded. In summary, we conservatively estimate that the data here have uncertainties of 1.0‰ for F1 and F2 fractions and 1.5‰ for F3. Uncertainty is greater for F3 because the abundant OSCs and other compounds in this fraction generated complex chromatograms with poorer baseline resolution. Although the analytical uncertainties are large compared with those typically achieved using conventional sulfur isotope analysis, they are nevertheless much smaller than the scale of isotopic variability observed in the Cariaco sulfur record and therefore still permit meaningful interpretation.

3.2. Analysis of bulk organic fractions using ICPMS

Aliquots of each fraction (F1, F2, F3) were dried and oxidized in 30% H₂O₂ at 90 °C for 24 h to convert OS to SO₄²⁻. Resulting SO₄²⁻ was purified on AG1-X8 anionic exchange resin according to the method described by Paris et al. (2013). Resin was washed with ten column volumes (CVs) 10% HNO₃, conditioned with 10 CVs 10% HCl and 10 CVs 0.5% HCl, loaded in trace HCl, and washed 3× with 5 CVs Milli-Q H₂O before SO₄²⁻ was eluted in 0.5 N HNO₃. SO₄²⁻ samples were quantified using ion chromatography (IC; Dionex ICS-2000) with an AS-19 anion column and AERS 500 ion regeneration. Concentrations were used to intensity-match samples and the required Na⁺ supplement for ICPMS analysis (Paris et al., 2013). Samples were injected into the plasma torch with a desolvating nebulizer (Aridus) and bracketed with known $\delta^{34}\text{S}$ NaSO₄ standards. The Neptune was operated in high resolution (M/ΔM ca. 10,000) to fully resolve oxygen interference on *m/z* 33 and 34. Accuracy was assessed by repeated analysis of a seawater SO₄²⁻ standard. Both accuracy and precision for $\delta^{34}\text{S}$ values in this mode of analysis were typically better than ± 0.2‰.

4. Results and discussion

4.1. Abundance and $\delta^{34}\text{S}$ of bulk OS

Concentrations of extractable OS polarity fractions and total residual OS ('kerogen' from Werne et al. (2003)) are shown in Fig. 1. In sediments, extractable OS increases with depth from 17 to 77 nmol S/g_{OC} and represents ca. 0.1‰ of residual OS. The $\delta^{34}\text{S}$ values of extractable and residual OS are similar, especially below 40 cm, and range from −18.0‰ to −25.9‰. Polar (F3) material represents 92–98% of total extractable OS.

4.2. OSC identification and abundance

A consistent suite of OSCs was observed with GC-MS-SCD and GC-ICP-MS at all sample depths. Two OSCs with well constrained EI mass spectra were assigned as isomers of a C₂₀ isoprenoid thiophene. They are inferred to derive from the sulfurization of phytol and/or phytadienes based on comparison with literature spectra (Brassell et al., 1986; Putschew et al., 1996). C₂₀ isoprenoid thiophenes have been widely observed in non-polar fractions of extracts from sediments (e.g. Sinninghe Damsté et al., 1987; Wakeham et al., 1995) and experimental studies (de Graaf et al., 1992; Rowland et al., 1993; Krein and Aizenshtat, 1994; Gelin et al., 1998). Here, two identical C₂₀ isoprenoid thiophenes were observed in multiple polarity fractions and could not be isolated in a single fraction using column chromatography. The sulfur isotopic composition of C₂₀ isoprenoids in the F1 and F3 fractions from the same sample is similar but not identical, and their concentration has a different trend with depth (Fig. 1; shaded compounds in panels A and B), consistent with the C₂₀ isoprenoid thiophenes in F1 and F3 having distinct precursors. Those in the non-polar fraction (F1), which are comparable to previous observations (e.g. Brassell et al., 1986; Fukushima et al., 1992), are interpreted to represent C₂₀ isoprenoid thiophenes present in the original sample. Because thiophenes can form at elevated temperature, we interpret the more abundant C₂₀ isoprenoid thiophenes in F3 as forming in the GC injector, for example via ring closure or aromatization of a more polar precursor with a similar phytol-derived skeleton. We find no evidence for either disulfide bonding or thiol groups in the precursors to the C₂₀ isoprenoid thiophenes in F3, and the original functional form of these molecules remains the subject of ongoing investigation.

Peaks eluting at 28 min were assigned as isomers of highly branched isoprenoid (HBI) thiolanes, presumably derived from the sulfurization of diatom HBI lipids. Mass spectra do not decisively establish whether the sulfur functionality is a thiolane or thiane, although the spectra share all major fragment ions with published HBI thiolane spectra (Kohnen et al., 1991). A single double bond in the molecule is indicated by the M⁺ ion at *m/z* 380. HBI thiolanes have been observed in Cariaco Basin sediments (Werne et al., 2000) and were isolated for conventional sulfur isotopic analysis (Werne et al., 2008). Similar to the C₂₀ isoprenoid thiophenes, identical HBI thiolanes were observed in both the apolar (F1) and polar (F3) fractions, with a higher abundance in F3 (5–63 nmol/g OC) than in F1 (2–18 nmol/g OC).

We also observed the monounsaturated triterpenoid thiane described previously from Cariaco Basin sediments based on published EI spectra (Wakeham et al., 1995; Werne et al., 2000) Its abundance here (6–69 nmol/g OC) is in the same range as observed previously (16–115 nmol/g OC; Werne et al., 2000).

One of the only volatile OSCs in F2 with a clear EI fragmentation spectrum (designated U-14) was tentatively assigned as a thiolane with twelve-carbons (C₁₂H₂₀S). The fragment at *m/z* 127 may represent C₇H₁₁S, which contains two double bond equivalents and

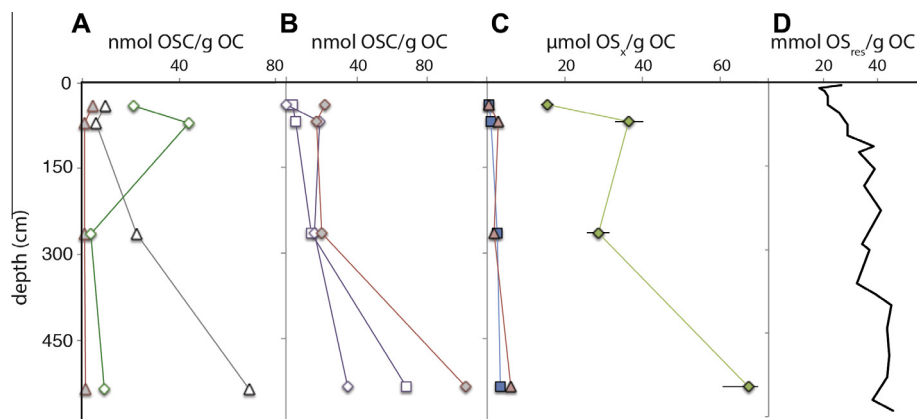


Fig. 1. Concentrations of individual OSCs and OS pools with depth in Cariaco sediments. Triangles, squares, and diamonds represent data associated with fractions F1, F2, and F3, respectively. (A) and (B) Concentration of individual OSCs. Panel A shows C_{20} isoprenoid thiophene (F1, shaded triangles), triterpenoid thiane (open triangles) and HBI thiolane (diamonds); these compounds are also highlighted in Fig. 2. Panel B shows a C_{20} isoprenoid thiophene (F3, shaded diamonds) and two unidentified compounds, U-14 (squares) and U-1 (diamonds). Panel C shows total extractable OS in F1 (triangles), F2 (squares) and F3 (diamonds); note scale change. Panel D shows concentration of residual OS. Note that this concentration is expressed relative to organic carbon (OC) rather than sediment mass. OC concentration averages 4.7 wt% throughout the core (data from Werne et al. (2003)).

appears to describe a thiane or thiolane aliphatic sulfide. Aliphatic sulfides are likely to fragment at the α - β carbon bond, leading us to infer the existence of a five carbon alkyl chain β to the sulfide sulfur.

We were also able to measure $\delta^{34}\text{S}$ values for nineteen other OSCs. These were observable with S-specific detectors like the ICPMS and GC-SCD but coeluted with much more abundant, non-S-bearing compounds in GC-MS. We were thus unable to obtain useful mass spectra despite attempting a variety of cleanup and fractionation schemes and different ionization methods (EI, CI, MS^2). Nevertheless, as shown in Fig. 2, these unidentified compounds have generally similar sulfur isotopic compositions, sug-

gesting that our assigned compounds are representative of the larger population of volatile OSCs.

The total amount of OSCs observed with GC-ICPMS was higher in F3 (83–306 nmol/g OC) than in F1 (34–117 nmol/g OC) or F2 (31–178 nmol/g OC). Individual compounds were present at a concentration of 1–100 nmol/g OC (Fig. 1). The triterpenoid thiane, unidentified compound U-14 and the C_{20} isoprenoid thiophene in F3 were particularly abundant at 535 cm, with concentrations of 68–102 nmol/g OC. Their concentrations were consistently lower in the shallower samples (4–20 nmol/g OC, Fig. 1B). In contrast, the concentrations of HBI thiolanes and C_{20} isoprenoid thiophenes in F1 dropped to relatively low values below maxima at 40 cm.

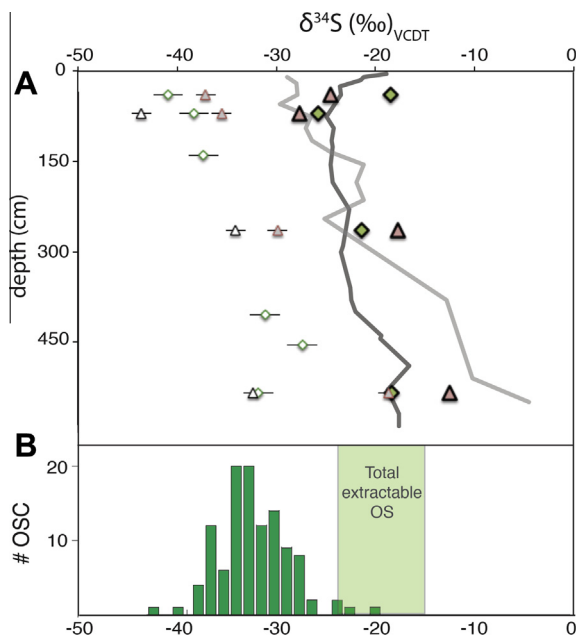


Fig. 2. Sulfur isotopic composition of OSCs and extractable OS fractions. Porewater sulfide (light gray line) and residual OS (dark gray line) data are from Lyons et al. (2003) and Werne et al. (2003). Panel A: Symbols with thick outlines indicate $\delta^{34}\text{S}$ values of total OS fractions F1 (triangles) and F3 (diamonds). Open symbols indicate $\delta^{34}\text{S}$ values of individual GC-amenable compounds in these fractions – triterpenoid thiane in F1 (open triangles), C_{20} isoprenoid in F1 (shaded triangles) and HBI thiolane in F3 (diamonds). Panel B: Histogram of all compound-specific measurements from Cariaco Basin sediment extracts, including both assigned and unidentified compounds. The shaded area represents the range of $\delta^{34}\text{S}$ measured for total extractable OS.

4.3. OSC sulfur isotopic composition

Several compounds have consistently lower $\delta^{34}\text{S}$ values than pyrite and represent the most highly ^{34}S -depleted species observed in the Cariaco Basin to date. In the shallowest sample, the triterpenoid thiane and HBI thiolane from F3 have $\delta^{34}\text{S}$ values of -43.6‰ and -40.9‰ , respectively, and less negative $\delta^{34}\text{S}$ values in deeper samples (between -32.3‰ and -28.2‰). C_{20} isoprenoid thiophenes from both F1 and F3 are more ^{34}S -enriched than the triterpenoid thiane and HBI thiolanes, with $\delta^{34}\text{S}$ values between -37.1‰ and -18.7‰ . Depth trends for these compounds are shown in Fig. 2A. Fig. 2B summarizes $\delta^{34}\text{S}$ values for all measured OSCs at all depths, including unidentified compounds. OSC $\delta^{34}\text{S}$ values have a unimodal distribution around ca. $-32 \pm 10\text{‰}$.

The sulfur isotopic compositions of HBI thiolanes in F1 and the triterpenoid thiane were measured in a previous study of Cariaco Basin sediment extracts by Werne et al. (2008). Using preparative liquid chromatography (LC) followed by EA-IRMS, they obtained $\delta^{34}\text{S}$ values between -21‰ and -5‰ for depths between 240 and 580 cm, an enrichment of ca. 30‰ relative to our GC-ICPMS results (Fig. 3). As these results apply to the same compounds, both cannot be correct. Given the improved specificity of our GC-ICPMS technique, the LC-EA-IRMS results probably described a mixture of the target OSC and some other coeluting (on LC) or background sulfur species, though there was no indication of additional compounds in the fraction when analyzed with GC-FPD (Werne et al., 2008). Nevertheless, the presence of a sulfur blank in the isolated fractions could potentially explain the high $\delta^{34}\text{S}$ values for OSCs in Werne et al. (2008), as these sulfur isotope compositions were determined via EA-IRMS.

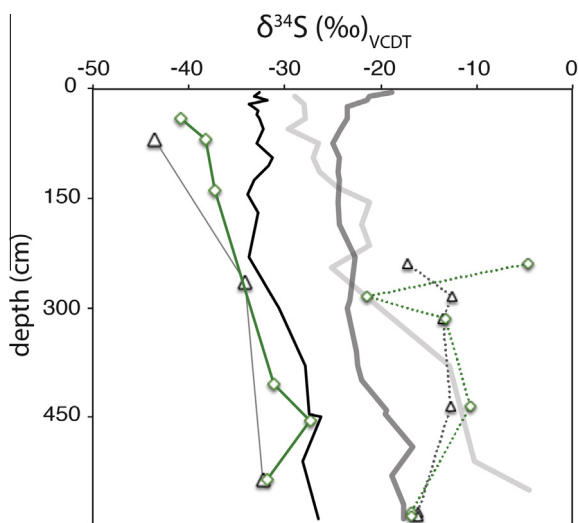


Fig. 3. Comparison of compound-specific $\delta^{34}\text{S}$ results from different analytical techniques. Sulfur isotopic composition of triterpenoid thiane (triangles) and HBI thiolane (diamonds) measured with two different analytical techniques. Symbols represent data obtained from GC-ICPMS (this study, smooth lines) and prep-LC and EA-IRMS (Werne et al., 2008, dashed lines). Lines without symbols represent residual OS (dark gray), porewater sulfide (light gray) and pyrite (black). ($\delta^{34}\text{S}$ values from Lyons et al., 2003, Werne et al., 2003).

4.4. Multiple timescales of OSC formation

Volatile OSCs in Cariaco Basin sediments have sulfur isotopic composition and depth profiles similar to coexisting pyrite (Fig. 3). A relatively large but variable proportion of sedimentary pyrite is formed in the water column (Lyons et al., 2003); this “syngenetic” pyrite forms in an effectively open system with respect to sulfide and its $\delta^{34}\text{S}$ value is affected by processes at the $\text{O}_2\text{-S}^{2-}$ interface. A smaller component of pyrite in Cariaco Basin sediments is diagenetic, forming in a diffusion-controlled regime within sediments in which sulfide $\delta^{34}\text{S}$ values increase with depth (Werne et al., 2003). Like pyrite, Cariaco OSCs are likely produced via both syngenetic and diagenetic processes. Different individual compounds may, however, preferentially form in one environment or the other. For example, Werne et al. (2000) demonstrated diagenetic production of the triterpenoid thiane based on the extent of precursor compound conversion. Consistent with the conclusions of that study, we find that the triterpenoid thiane increases in concentration from 5.7 to 69 nmol/g OC as its $\delta^{34}\text{S}$ value increases from -43.6‰ to -32.3‰ . Both concentration and sulfur isotope data thus support predominantly diagenetic formation of this compound. C_{20} isoprenoid thiophenes in F3 and compound U-14 also have similar concentration profiles with only slightly smaller shifts in their $\delta^{34}\text{S}$ values between 70 and 535 cm (Fig. 1). Thus they are also probably products of sedimentary diagenesis, forming on a timescale of thousands of years.

In contrast, other OSCs exhibit no concentration change with depth, thereby providing no conclusive evidence for accumulation during diagenesis. Nevertheless, the $\delta^{34}\text{S}$ values of HBI thiolanes from F3, C_{20} isoprenoid thiophene from F1, and compound U-1 also increase by 7–10‰ over the 6 m core, comparable with the pattern observed for diagenetic OSCs and implying ongoing formation. Concentration and $\delta^{34}\text{S}$ profiles for these compounds can be reconciled in one of two ways. First, they may have a significant syngenetic source, with their concentration profiles reflecting variable production in the water column over time. Isotopic variability on the scale of a few permil would then reflect dynamic sulfur cycling near the chemocline, where sulfide $\delta^{34}\text{S}$ can vary due to changes in local redox state (Li et al., 2010, 2011). Alternatively, changes in the $\delta^{34}\text{S}$ values of non-accumulating OSCs with depth could result from

slow equilibration between the OSCs and (poly)sulfides. Given the scale of depositional variability evident in the core, either scenario seems viable.

4.5. Isotope effects during OM sulfurization

The $\delta^{34}\text{S}$ profiles for individual OSCs in Cariaco Basin reflect a combination of the $\delta^{34}\text{S}$ values of the reactant sulfur species, the mechanism of sulfurization and any associated fractionation during incorporation. Our results help constrain the possible mechanisms of OM sulfurization in Cariaco sediments.

Both bisulfide and polysulfide species have been considered probable reactants for sulfurization (Anderson and Pratt, 1995). Under typical sedimentary conditions, the dominant species available to react with OM are the bisulfide anion (HS^-) and dianionic polysulfide (S_x^{2-} ; Schwarzenbach and Fischer, 1960). The same species are involved in pyrite formation (Rickard and Luther, 2007), which occurs at a low rate in Cariaco sediments (Lyons et al., 2003; Werne et al., 2003). In Cariaco sediment porewater, the $\delta^{34}\text{S}$ value of dissolved HS^- increases from -29‰ near the sediment–water interface to $> -5\text{‰}$ at 550 cm depth. Thus, all of the volatile OSCs we observe are more ^{34}S -depleted than coexisting dissolved HS^- , their likely sulfur source. The $\delta^{34}\text{S}$ difference between porewater sulfide and coexisting OSCs is as much as 17‰ (triterpenoid thiane, 70 cm). Polysulfide $\delta^{34}\text{S}$ has not been measured directly in Cariaco Basin, but experimental work has documented a small ^{34}S enrichment in polysulfides relative to total sulfur at equilibrium (Amrani et al., 2006). We thus predict that polysulfides are slightly more ^{34}S -enriched than HS^- in Cariaco Basin, so the apparent kinetic isotope effect associated with OSC formation from polysulfides would be even larger than for HS^- . We also note that oxidants are limiting in Cariaco sediments (Lyons et al., 2003), which should maintain very low polysulfide concentration and potentially favor OM sulfurization reactions involving plentiful HS^- .

If we assume that porewater (poly)sulfide is the source of sulfur for these ^{34}S -depleted OSCs, their formation would appear to involve a normal kinetic isotope effect, i.e. the reaction between (poly)sulfide and an organic molecule proceeds more rapidly for the lighter S isotope. A normal kinetic isotope effect has been predicted for initial C–S bond formation (Brüchert and Pratt, 1996) during sedimentary OM sulfurization. In contrast, an equilibrium isotope effect would result in ^{34}S -enrichment in the compound with the stronger bond and would be expected to produce OSCs enriched in ^{34}S relative to (poly)sulfides (Amrani et al., 2004a). Reversible reactions should lead to an isotopic composition governed by equilibrium isotope effects, whereas irreversible reactions typically record kinetic isotope effects (Hayes, 1993). Therefore, the sulfurization reactions leading to extractable OSC monomers in Cariaco sediments may be largely irreversible.

Sulfur addition by HS^- is more likely to be irreversible than versus sulfur addition by S_x^{2-} . Initial nucleophilic attack by a HS^- on an organic functional group produces a thiol. In contrast, the initial product of nucleophilic attack by a S_x^{2-} has a chain of two or more sulfur atoms that retain a negative charge. These products may subsequently undergo reaction with another functional group, either on the same molecule, forming a ring, or on a different molecule, forming a (poly)sulfide bridge (Fig. 4). Rapid intramolecular addition would be more energetically favorable for a HS^- -derived thiol group than for a S_x^{2-} chain due to the relative strength of the S–S bond compared with the S–H bond. It is likely – although not certain for compounds appearing in multiple fractions – that all of the volatile compounds we identified in Cariaco lipid extracts experienced intramolecular addition for that second step. Therefore, if we assume that volatile OSC monomers in Cariaco Basin derive from either porewater S_x^{2-} or HS^- , their highly ^{34}S -depleted

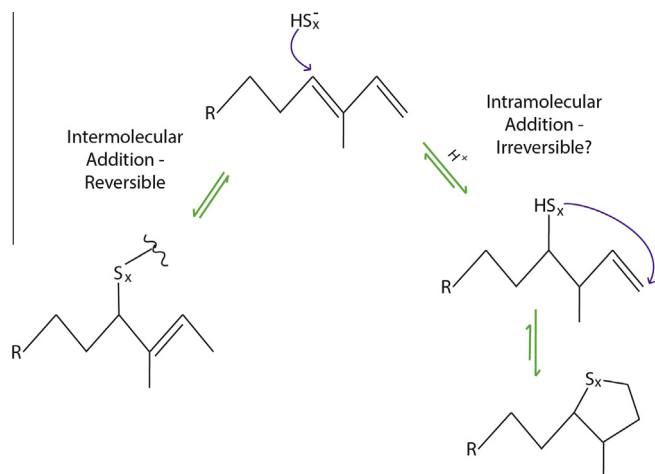


Fig. 4. Examples of intermolecular and intramolecular sulfuration pathways following initial (poly)sulfide attack on a diene. Based on Kohnen et al. (1990).

isotopic compositions appear to derive from the HS^- anion and a strong kinetic isotope effect.

A large kinetic isotope effect has not been reported for OM sulfuration. Total residual OS is typically more ^{34}S -enriched than its sulfur source, broadly indicating an equilibrium isotope effect in its formation. This relationship holds both in a global compilation of rocks, where pyrite $\delta^{34}\text{S}$ is taken to represent HS^- (Bottrell and Raiswell, 2000) and in modern marine sediments (Dale et al., 2009). However, individual OSCs need not conform to models based on total OS. In Cariaco Basin, both extractable and residual OS, which are similar below 70 cm, are significantly more ^{34}S -enriched than the GC-amenable OSCs separated from the extractable OS pool. Thus, extractable OS in Cariaco Basin must represent a mixture of OS with distinct S-isotopic compositions.

Based on the above evidence, we propose that OM sulfuration may be associated with equilibrium or kinetic isotope effects under different conditions (Fig. 4). Although all of the volatile OSCs measured here with GC-ICP-MS fall into the second category, there is evidence for both types of isotope effect in the basin. The formation of GC-amenable OSCs in the basin also appears to precede sulfur incorporation into residual OS, because all of the major species of volatile OSCs are abundant by 40 cm depth, whereas lipid sulfur cross-linking remains minimal at 27 cm (Aycard et al., 2003). Different timescales for the onset of bitumen OSCs and sulfurized polymer formation are also consistent with a mechanistic distinction between reversible and irreversible sulfuration pathways.

Alternatively, volatile OSCs could potentially form with an equilibrium isotope effect if they derive from a S_x^{2-} pool that has a different isotopic composition from porewater HS^- . Such an isolated pool would need to be substantially more ^{34}S -depleted than porewater HS^- and might be present within cells or in microenvironments in the sediment. Without corroborating evidence for the existence of such an isolated reservoir, this explanation remains speculative. Still, if their existence is supported by future work, non-porewater S_x^{2-} reactants could explain OSCs with $\delta^{34}\text{S}$ values that differ from porewater S^{2-} $\delta^{34}\text{S}$ without invoking a large kinetic isotope effect during OSC formation.

The hypothesized distinction between the $\delta^{34}\text{S}$ values of the products of inter- and intramolecular sulfuration may provide a useful constraint on the processes controlling kerogen formation and a path toward a better understanding of the preservation of OC within the kerogen matrix. Previous attempts at interpreting the sulfur isotopic composition of bulk sedimentary OM have suffered from analytical limitations (Wakeham et al., 1995; Werne et al., 2008), presenting a serious impediment to

paleoenvironmental studies that rely on sulfur isotopic signals or preserved biomarkers in kerogen to reconstruct paleoenvironmental conditions. Different sulfuration mechanisms may yield distinct isotopic fractionations that will have different effects on sulfur isotope mass balance and on the isotopic signals preserved in sedimentary records. This study is, in part, a proof of concept that should guide future efforts.

5. Conclusions

The sulfur isotopic composition of GC-amenable OSCs in Cariaco Basin sediments ranges from -43.6‰ to -18.7‰ , similar to coexisting pyrite but more ^{34}S -depleted than total extractable and residual OS. OM sulfuration in the basin appears to occur on multiple timescales. Concentration increases and ^{34}S enrichment with depth reflect primarily diagenetic production on kyr timescales for a triterpenoid thiane, C_{20} isoprenoid thiophene in polar extracts (F3) and unidentified compound U-14, while either variable syngenetic sources or diagenetic sinks exist for HBI thiolanes in both polar and non-polar extracts (F1 and F3), C_{20} isoprenoid thiophene in non-polar extracts (F1) and compound U-1. Regardless of their concentration patterns, all the compounds exhibit a normal kinetic isotope effect relative to their reactant sulfur source, which is most likely porewater HS^- . This hypothesis contrasts with the equilibrium isotope effects observed for the formation of sulfur cross-linked OSC polymers from S_x^{2-} (Amrani and Aizenshtat, 2004a,b) and with the incorporation of (apparently) similar sulfur species into kerogen in the basin (Aycard et al., 2003). We hypothesize that at least two distinct pathways are at work in generating sedimentary OSCs and that they may be distinguished via their sulfur isotopic composition. If correct, compound-specific $\delta^{34}\text{S}$ analysis of OSCs should provide a powerful tool for unraveling the complex pathways of kerogen formation.

Acknowledgments

We thank N. Dalleska and G. Paris at Caltech for significant analytical assistance, and J. Rae, A. Amrani, C. Marotta and A. Subhas for helpful advice. We also thank two anonymous reviewers, whose comments significantly improved the manuscript. Financial support was provided by the National Science Foundation through award EAR-1024919 to A.L.S. and J.F.A. The research is also funded in part by the Gordon and Betty Moore Foundation through Grant GBMF#3306 to A.L.S.

Appendix A. Supplementary data

Supplementary data associated with this article can be found, in the online version, at <http://dx.doi.org/10.1016/j.orggeochem.2015.01.002>.

Associate Editor—S. Schouten

References

- Aizenshtat, Z., Krein, E., Vairavamurthy, M.A., Goldstein, T., 1995. Role of sulfur in the transformations of sedimentary organic matter: a mechanistic overview. In: *Geochemical Transformations of Sedimentary Sulfur*. ACS Symposium Series 612. Washington, DC, pp. 16–37.
- Amrani, A., Aizenshtat, Z., 2004a. Mechanisms of sulfur introduction chemically controlled: $\delta^{34}\text{S}$ imprint. *Organic Geochemistry* 35, 1319–1336.
- Amrani, A., Aizenshtat, Z., 2004b. Reaction of polysulfide anions with α , β unsaturated isoprenoid aldehydes in aquatic media: simulation of oceanic conditions. *Organic Geochemistry* 35, 909–921.
- Amrani, A., Deev, A., Sessions, A., Tang, Y., Adkins, J., Hill, R., Moldowan, M., Wei, Z., 2012. The sulfur-isotopic compositions of benzothiophenes and dibenzothiophenes as a proxy for thermochemical sulfate reduction. *Geochimica et Cosmochimica Acta* 84, 152–164.

- Amrani, A., Kamysnyh Jr., A., Lev, O., Aizenshtat, Z., 2006. Sulfur stable isotope distribution of polysulfide anions in an $(\text{NH}_4)_2\text{S}$ aqueous solution. *Inorganic Chemistry* 45, 1427–1429.
- Amrani, A., Sessions, A., Adkins, J., 2009. Compound-specific $\delta^{34}\text{S}$ analysis of volatile organics by coupled GC/multicollector-ICPMS. *Analytical Chemistry* 81, 9027–9034.
- Anderson, T.F., Pratt, L.M., 1995. Isotopic evidence for the origin of organic sulfur and elemental sulfur in marine sediments. In: *Geochemical Transformations of Sedimentary Sulfur*. ACS Symposium Series 612, Washington, DC, pp. 378–396.
- Aycard, M., Derenne, S., Largeau, C., Mongenot, T., Tribouvillard, N., Baudin, F., 2003. Formation pathways of proto-kerogens in Holocene sediments of the upwelling influenced Cariaco Trench, Venezuela. *Organic Geochemistry* 34, 701–718.
- Bottrell, S.H., Raiswell, R., 2000. Sulphur isotopes and microbial sulphur cycling in sediments. In: Riding, R., Awramik, S. (Eds.), *Microbial Sediments*. Springer, Berlin Heidelberg, pp. 96–104.
- Brassell, S.C., Lewis, C.A., De Leeuw, J.W., de Lange, F., Damsté, J.S., 1986. Isoprenoid thiophenes: novel products of sediment diagenesis? *Nature* 320, 160–162.
- Brüchert, V., Pratt, L.M., 1996. Contemporaneous early diagenetic formation of organic and inorganic sulfur in estuarine sediments from St. Andrew Bay, Florida, USA. *Geochimica et Cosmochimica Acta* 60, 2325–2332.
- Dale, A.W., Brüchert, V., Alperin, M., Regnier, P., 2009. An integrated sulfur isotope model for Namibian shelf sediments. *Geochimica et Cosmochimica Acta* 73, 1924–1944.
- Damsté, J., Rijpstra, I., Coolen, M., Schouten, S., Volkman, J., 2007. Rapid sulfurisation of highly branched isoprenoid (HBI) alkenes in sulfidic Holocene sediments from Ellis Fjord, Antarctica. *Organic Geochemistry* 38, 128–139.
- Damsté, J.S.S., De Leeuw, J.W., 1990. Analysis, structure and geochemical significance of organically-bound sulphur in the geosphere: state of the art and future research. *Organic Geochemistry* 16, 1077–1101.
- Damsté, J.S.S., De Leeuw, J.W., Dalen, A.K.-V., de Zeeuw, M.A., de Lange, F., Rijpstra, W., Schenck, P.A., 1987. The occurrence and identification of series of organic sulphur compounds in oils and sediment extracts. I. A study of Rozel Point Oil (U.S.A.). *Geochimica et Cosmochimica Acta* 51, 2369–2391.
- de Graaf, W., Damsté, J.S., De Leeuw, J.W., 1992. Laboratory simulation of natural sulphurization: I. Formation of monomeric and oligomeric isoprenoid polysulphides by low-temperature reactions of inorganic polysulphides with phytol and phytadienes. *Geochimica et Cosmochimica Acta* 56, 4321–4328.
- Eglinton, T.I., Irvine, J.E., Vairavamurthi, Zhou, W., Manowitz, B., 1994. Formation and diagenesis of macromolecular organic sulfur in Peru margin sediments. *Organic Geochemistry* 22, 781–799.
- Francois, R., 1987. A study of sulphur enrichment in the humic fraction of marine sediments during early diagenesis. *Geochimica et Cosmochimica Acta* 51, 17–27.
- Fukushima, K., Yasukawa, M., Muto, N., Uemura, H., Ishiwatari, R., 1992. Formation of C_{20} isoprenoid thiophenes in modern sediments. *Organic Geochemistry* 18, 83–91.
- Gelin, F., Kok, M.D., De Leeuw, J.W., Damsté, J.S.S., 1998. Laboratory sulfurisation of the marine microalga *Nannochloropsis salina*. *Organic Geochemistry* 29, 1837–1848.
- Hayes, J., 1993. Factors controlling ^{13}C contents of sedimentary organic compounds: principles and evidence. *Marine Geology* 113, 111–125.
- Kohnen, M.E.L., Damsté, J.S., Kock-van Dalen, A.C., Ten Haven, H.L., Rullkötter, J., De Leeuw, J.W., 1990. Origin and diagenetic transformations of C_{25} and C_{30} highly branched isoprenoid sulphur compounds: Further evidence for the formation of organically bound sulphur during early diagenesis. *Geochimica et Cosmochimica Acta* 54, 3053–3063.
- Kohnen, M.E.L., Damsté, J.S., Dalen, A.C.K.-V., Haven, H.L.T., Rullkötter, J., De Leeuw, J.W., 1990. Origin and diagenetic transformations of C_{25} and C_{30} highly branched isoprenoid sulphur compounds: further evidence for the formation of organically bound sulphur during early diagenesis. *Geochimica et Cosmochimica Acta* 54, 3053–3063.
- Kok, M., Schouten, S., Damsté, J.S., 2000. Formation of insoluble, nonhydrolyzable, sulfur-rich macromolecules via incorporation of inorganic sulfur species into algal carbohydrates. *Geochimica et Cosmochimica Acta* 64, 2689–2699.
- Krein, E.B., Aizenshtat, Z., 1994. The formation of isoprenoid sulfur compounds during diagenesis: simulated sulfur incorporation and thermal transformation. *Organic Geochemistry* 21, 1015–1025.
- Li, X., Cutter, G.A., Thunell, R.C., Tappa, E., Gilhooly III, W.P., Lyons, T.W., Astor, Y., Scranton, M.I., 2011. Particulate sulfur species in the water column of the Cariaco Basin. *Geochimica et Cosmochimica Acta* 75, 148–163.
- Li, X., Gilhooly III, W.P., Zerkle, A.L., Lyons, T.W., Farquhar, J., Werne, J.P., Varela, R., Scranton, M.I., 2010. Stable sulfur isotopes in the water column of the Cariaco Basin. *Geochimica et Cosmochimica Acta* 74, 6764–6778.
- Lin, H., Peterson, L., Overpeck, J., Trumbore, S., Murray, D., 1997. Later Quaternary climate change from $\text{d}18\text{O}$ records of multiple species of planktonic foraminifera: High-resolution records from the anoxic Cariaco Basin, Venezuela. *Paleoceanography* 12, 415–427.
- LaLonde, R., Ferrara, L., Hayes, M., 1987. Low-temperature, polysulfide reactions of conjugated ene carbonyls: a reaction model for the geologic origin of S-heterocycles. *Organic Geochemistry* 11, 563–571.
- Lyons, T.W., Werne, J.P., Hollander, D.J., Murray, R.W., 2003. Contrasting sulfur geochemistry and Fe/Al and Mo/Al ratios across the last oxic-to-anoxic transition in the Cariaco Basin, Venezuela. *Chemical Geology* 195, 131–157.
- Paris, G., Sessions, A., Subhas, A., Adkins, J., 2013. MC-ICP-MS measurement of $\delta^{34}\text{S}$ and D^{33}S in small amounts of dissolved sulfate. *Chemical Geology* 345, 50–61.
- Putschew, A., Scholz-Böttcher, B.M., Rullkötter, J., 1996. Early diagenesis of organic matter and related sulphur incorporation in surface sediments of meromictic Lake Cadagno in the Swiss Alps. *Organic Geochemistry* 25, 379–390.
- Rickard, D., Luther, G.I., 2007. Chemistry of iron sulfides. *Chemical Reviews* 107, 514–562.
- Rowland, S., Rockey, C., Al-Lihaibi, S.S., Wolff, G.A., 1993. Incorporation of sulphur into phytol derivatives during simulated early diagenesis. *Organic Geochemistry* 20, 1–5.
- Schmid, J.C., Connan, J., Albrecht, P., 1987. Occurrence and geochemical significance of long-chain dialkylthiacyclopentanes. *Nature* 329, 54–56.
- Schouten, S., de Graaf, W., Damsté, J.S., van Driel, G., De Leeuw, J.W., 1994. Laboratory simulation of natural sulphurization: II. Reaction of multifunctionalized lipids with inorganic polysulphides at low temperatures. *Organic Geochemistry* 22, 825–834.
- Schwarzenbach, G., Fischer, A., 1960. Die acidität der sulfane und die zusammensetzung wässriger polysulfidlösungen. *Helvetica Chimica Acta* 43, 1365–1390.
- Shipboard Scientific Party, 1997. In: *Proceedings of the Ocean Drilling Program, Initial Reports*. College Station, TX.
- Vairavamurthy, A., Mopper, K., 1987. Geochemical formation of organosulphur compounds (thiols) by addition of HS to sedimentary organic matter. *Nature* 329, 623–625.
- Vairavamurthy, A., Zhou, W., Eglinton, T., Manowitz, B., 1994. Sulfonates: a novel class of organic sulfur compounds in marine sediments. *Geochimica et Cosmochimica Acta* 58, 4681–4687.
- Vandenbroucke, M., Largeau, C., 2007. Kerogen origin, evolution and structure. *Organic Geochemistry* 38, 719–833.
- Wakeham, S., Damsté, J.S., Kohnen, M., De Leeuw, J.W., 1995. Organic sulfur compounds formed during early diagenesis in Black Sea sediments. *Geochimica et Cosmochimica Acta* 59, 521–533.
- Werne, J., Hollander, D., Behrens, A., Schaeffer, P., Albrecht, P., Damsté, J., 2000. Timing of early diagenetic sulfurization of organic matter: a precursor-product relationship in early Holocene sediments of the anoxic Cariaco Basin, Venezuela. *Geochimica et Cosmochimica Acta* 65, 1741–1751.
- Werne, J., Lyons, T., Hollander, D., Formolo, M., Damsté, J., 2003. Reduced sulfur in euxinic sediments of the Cariaco Basin: sulfur isotope constrains on organic sulfur formation. *Chemical Geology* 195, 159–179.
- Werne, J., Lyons, T., Hollander, D., Schouten, S., Hopmans, E., Damsté, J., 2008. Investigating pathways of diagenetic organic matter sulfurization using compound-specific sulfur isotope analysis. *Geochimica et Cosmochimica Acta* 72, 3489–3502.